

Design and Fabrication of a Two-Port Three-Beam Switched Beam Antenna Array for 60 GHz Communication

 ISSN 1751-8644
doi: 0000000000
www.ietdl.org

 Yuqiao Liu¹, Oday Bshara¹, Ibrahim Tekin², Christopher Israel³, Ahmad Hoorfar³, Baris Taskin¹, Kapil R. Dandekar¹
¹ Electrical and Computer Engineering Department, Drexel University, 3141 Chestnut Street, Philadelphia, PA, 19104, USA

² Electronics Engineering, Sabanci University, 34956 Orhanli, Istanbul, Turkey

³ ECE Department, Villanova University, Villanova, PA, 19085, USA

 * E-mail: y1636, ob67, bt62, krd26@drexel.edu¹, tekin@sabanciuniv.edu², cisrael, ahmad.hoorfar@villanova.edu³

Abstract: This letter presents a novel, low-cost, beam-switchable 2×10 antenna array system operating at 60 GHz. This antenna system is constructed of two rows of Chebyshev tapered microstrip antenna arrays. Each row is a 10 element series-fed array which are fed by a 90° coupler. The designed antenna array has only two input ports, but it is capable of generating three switchable beams. This antenna system can spatially scan 90° with at least -5dB normalized gain using only one SPDT switch and a single transceiver. The maximum gain realized by the system was measured as 16.4 dBi and the bandwidth (BW) was more than 1 GHz. The features of the proposed antenna system make it applicable to do mmWave research such as beamforming algorithms and channel sounding, and to use in handsets for 5G communication.

1 Introduction and Related Work

The massive growth of mobile data and the increasing demand for higher data rates that exceed the channel capacity of 4G and LTE (Long Term Evolution) [1] have motivated next generation (5G) cellular systems. New technologies such as cell densification, massive MIMO, and mmWave are forming the backbone of 5G. Regarding mmWave spectrum, high gain and beam steerable antenna arrays are necessary to overcome significant free space path loss, atmospheric attenuation, and blockage by foliage at high frequencies [2] [3].

Smart antenna systems, including switched-beam systems and adaptive array systems, both can be electronically steered to point in different directions without physically moving the antennas. Smart antenna systems are the key technology to tackle the challenges in mmWave bands. On one hand, adaptive array systems are able to fully adapt to mobile channel environments in real time by generating an optimal radiation pattern that can maximize their main lobe and minimize interference. On the other hand, switched beam systems are fed by an analog beamformer which requires a smaller number of transceivers, resulting in reduced system complexity and cost.

Given the pros and cons of analog and digital beamforming, there should be a trade-off in order to balance between performance with real-time signal processing, power consumption, cost and system complexity by utilizing hybrid beamforming[4], in which a switched-beam antenna array acts as a subsystem[5] [6]. Passive multibeam arrays (PMBAs) based on beam forming circuits are much less complex compared with phase-shifter based switched-beam antennas[7] and the array deploying the local oscillator (LO) phase-shifting approach. However, when the user position is between two adjacent beams, corresponding selection rules and possible SINR reduction need to be taken into account[3].

Usually, an $N \times N$ beamforming network with N inputs and N outputs can only generate N beams. The work in [8][9] [10] used a 4×4 butler matrix to generate 4 fixed beams. Other previous works [11] [12] designed 3×3 beamformers that have enabled 3 direction beamforming with much simpler hardware. However, they needed more than two hybrid couplers and several phase shifters to implement the three-port beamforming network. When the number of input ports comes down to only two, beamforming networks

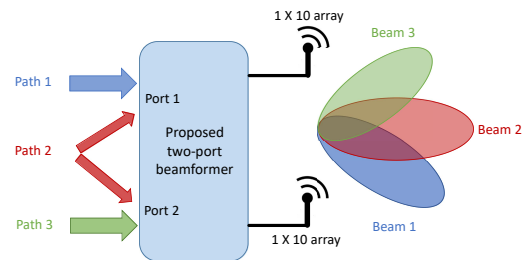


Fig. 1: An overview diagram of the proposed antenna array system. Each antenna symbol stands for a 1×10 antenna array. Feeding through port 1 results in Beam 1. Feeding through port 2 results in Beam 3. Signal is fed to both ports to generate Beam 2.

become a 90° hybrid coupler which produces two outputs with a phase increment of $\pm 90^\circ$.

In this paper, we designed a low complexity 60 GHz antenna system for 5G mobile user equipment (UE). Previous research generated only M beams out of a $M \times N$ array, which means that, using this approach, one would need a $3 \times N$ array to generate 3 beams and a 4 by N array to generate 4 beams. The novelty of our solution allows for the generation of 3 beams from a simple $2 \times N$ array. The solution can potentially be extended to generating $M \times 2$ beams out of a $M \times N$ array. Our design has a feeding circuit with an uncommon use of an SPDT switch. Usually, a SPDT switch is connected to one of the outputs at a time. However, our switch has an additional state when both control bins are enabled at the same time. This state generates the additional third beam. Figure 1 depicts the generated beams. When we feed the system at port 1 we get Beam 1. When we feed the system at port 2 we generate Beam 3. When we divide the input signal power and pass it into ports 1 and 2 we get Beam 2. The feeding network outputs are 0° , or $\pm 90^\circ$ phase difference. Then, the signals with the proper magnitude and phase difference

propagate into a two-row series-fed microstrip antenna array with 10 elements each working at 60 GHz in order to achieve the high gain that mmWave communication requires.

The remaining parts of this paper are organized as below: section 2 is a system overview, section 3 describes our antenna design and the fabrication process, section 4 depicts the measurements and the antenna performance, section 5 concludes our work.

2 System Overview

It is well known that the circuit of a quadrature hybrid coupler can be decomposed into the superposition of an even-mode and an odd-mode excitation [13]. When excited from a single port, the coupler is working at both modes, making the other input port isolated. When excited from both ports by the same signal, the coupler is working at even-mode only. The symmetric structure and even mode excitation produce a virtual open circuit at the center of Z_0 stubs which separates the two signal paths. Therefore, at the output ends, both output signals having the same magnitude and phase, produce an RF signal with 0° phase difference fed to the antenna arrays.

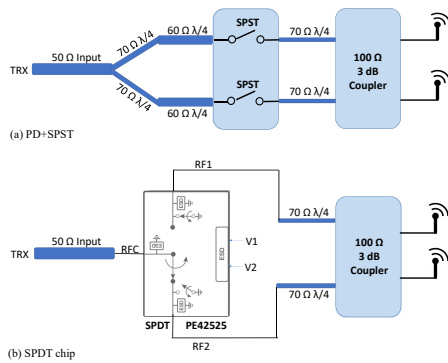


Fig. 2: Power divider and SPDT setup structure to generate 3 beams out of 2 antenna arrays. Every antenna element symbol represents a 1×10 antenna array.

Switching circuits are designed to switch among different excitation modes to generate the three beams. There are two possible switching circuit solutions: as shown in Figure 2: First option is to use a power divider (PD) and two SPST switches. This design leaves one of the output ports of the PD as an open circuit. In order to deal with this open circuit issue we extended the outputs of the PD by 60Ω quarter-wavelength transmission lines before connecting it to the SPST in order to ensure that, for the PD, the insertion loss is (-1 dB) and the reflection coefficient is (-15 dB). Second, the circuit in Figure 3 uses commercially available SPDT switch chips such as PE42525 from Peregrine Semiconductor[14]. Figure 3 shows the principle of operation: When only one of the control signals V1 or V2 is high, the antenna system is able to generate beam 1 or beam 3; When the control signals V1 and V2 are both high, the RF paths 1 and 2 are all turned on according to the truth table from the datasheet of PE42525 chip. Thus, the signal is fed to both input ports, generating beam 2.

3 Design and Fabrication

The antenna system was designed based on microstrip transmission lines (MTLs). In order to reduce the fabrication cost, no vias were needed except for the connector-mounting area. Considering

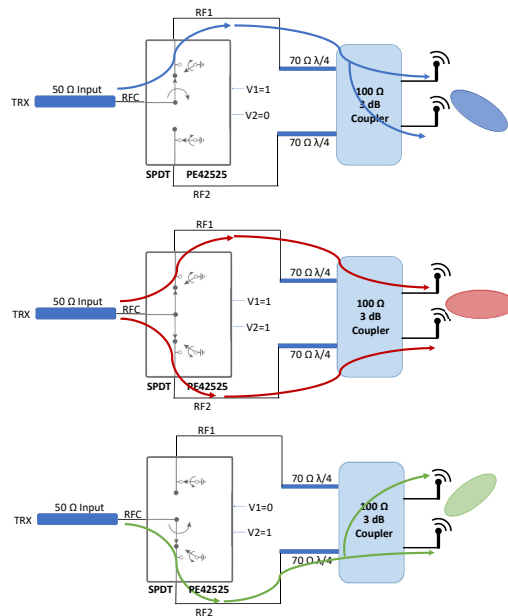


Fig. 3: SPDT setup structure to generate 3 beams out of 2 antenna arrays. Every antenna element symbol represents a 1×10 antenna array. Color scheme is the same as the one in Figure 1. Each color represents one switching option that generates a beam.

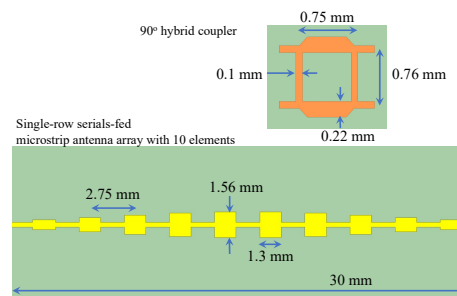


Fig. 4: Dimensions of 90° hybrid coupler and single row antenna array.

both cost and loss, two-layer 0.2 mm (8mil) thickness RO4003 laminate was selected as a substrate which was thin enough to avoid any unexpected higher order modes and surface waves. The design initially ran through an extensive simulation process for its critical components such as the 90° coupler, the single patch antenna, and the single row 1×10 antenna array with the help of ANSYS High Frequency Structure Simulator (HFSS) version 19.1.

The dimension and structure of the key components are shown in Figure 4. The coupler was designed using $Z_0=100\Omega$ characteristic impedance system. This Z_0 choice was made after comparing the quarter wavelength of 100Ω and 50Ω MTLs. 50Ω quarter wavelength MTL would have been large and would have caused coupling between transmission lines.

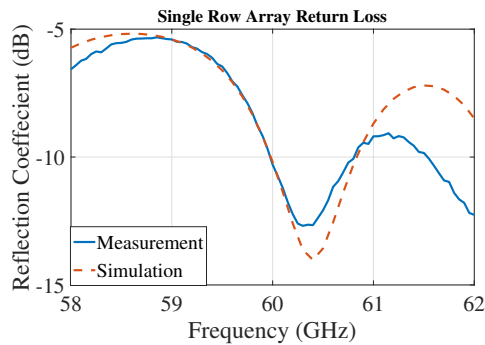


Fig. 5: Comparison of simulated and measured return loss of a 1 × 10 array.

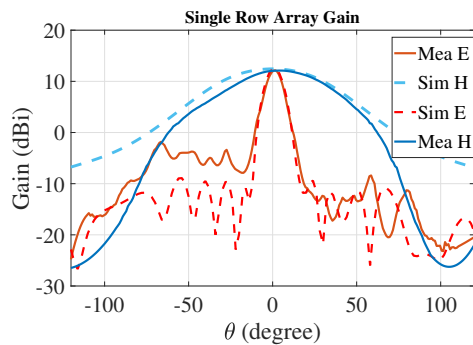


Fig. 6: Comparison of simulated and measured gain of a 1 × 10 array at 60.4GHz

Series-fed microstrip antennas are commonly used due to their simple feed line compared with complex corporate-fed networks. We first designed a single half-wavelength patch operating at 60 GHz. Then, in order to implement 50Ω input impedance, we took advantage of the high propagation loss at mmWave band to feed the patches from the edges by half-wavelength MTLs. After connecting the first element to the other 9 half-wavelength patches and 9 half-wavelength MTLs, the whole structure stays resonant at 60 GHz, but the resonant impedance reduces from 300Ω[13], with only one element, to 50Ω with 10 elements as the return loss plot shows in Figure 5. Then, the widths of each patch are tapered using Chebyshev polynomials for equal side lobe level in magnitude. The tapering ratio is 1 : 0.91 : 0.74 : 0.54 : 0.38 from the center patch to edge to ensure that the side-lobe level is 20 dB lower than the main beam in the E plane. We used 1.3 mm for the length of patch elements, 0.1 mm shorter than half-wavelength due to the fringing fields near the edge of each patch, we also used approximately half-wavelength (1.45 mm) long, 0.3 mm wide MTLs to connect patches together. The distance between adjacent patch elements is 2.75 mm, which is about 0.55 wavelength in the air. The performance of the single-row array was validated before taking the measurements of the whole system. The reflection coefficient plots in Figure 5 shows 1 GHz -10 dB bandwidth and Figure 6 plots the antenna gain in both E and H planes, showing a maximum gain of 12.14 dBi at 60.4 GHz.

Although a two layer board can be used for fabrication, we decided to use a four layer stacked structure in order to enhance mechanical strength. The stack structure of the PCB is shown in 7: the first layer is half oz copper for the transmission lines and patches, the second copper layer is a whole ground plane made with half oz

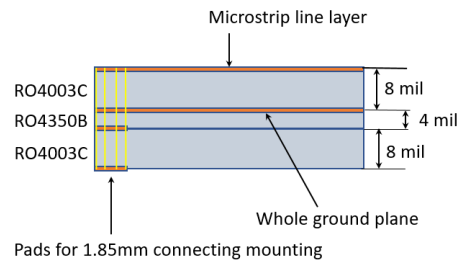
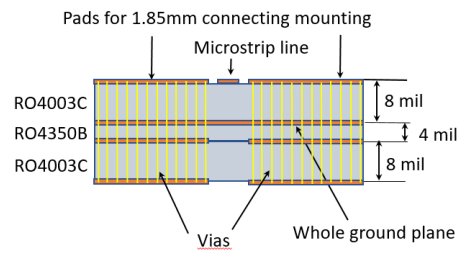


Fig. 7: Front view (top) and side view(bottom) of 4-layer PCB stack structure

copper, while the third and fourth layers have copper only for connector mounting. 8 mil RO4003C laminate was used between the first and second layers as well as between the third and fourth layers. We used 4 mil thick RO4350B between the second and the third layers. Electroless Nickel with Immersion Gold coating (ENIG) was chosen as a surface finishing process for the purpose of avoiding corrosion. Figure 9 shows the fabricated two row antenna connected to the output of a coupler.

4 Performance of Antenna System

In order to evaluate the performance of our design we initially characterized port isolation and return loss by collecting S parameter measurements of the 2 × 10 array using a Keysight PNA-X N5247 10MHz-67GHz network analyzer in the Drexel Wireless Systems Laboratory (DWSL). Figure 10 shows less than -15 dB return loss from 59 GHz to 62 GHz as well as below -15 dB isolation between input ports from 59.5 GHz to 61.5 GHz.

Radiation performances of the proposed antenna system were measured in the anechoic chamber (compact range) of the Antenna Research Laboratory (ARL) at Villanova University. The measurement device under test (DUT) comprises the fabricated 2 × 10 antenna array connected to the 90° coupler, two Southwest 1892-04A-6 1.85 mm End Launch Low Profile connectors, coaxial cables, and a Pulsar PS2-57-450/15S two way power divider. Insertion loss of the components other than the antenna system was compensated for through measurement system calibration.

From the anechoic chamber measurements shown in Figure 10 (right), we can see the maximum system gain is over 12 dBi covering the frequency range from 59.5GHz-61.3GHz, while maximum gain was 12.93 dBi at 60.2 GHz. The simulated and measured radiation patterns of E and H planes are presented in Figures 11 and 12 respectively. It can be seen in the E plane, side lobes on the right side are -20 dB less than the main lobe thanks to the tapering technique. The side lobes at the left side are a little bit higher due to the spurious radiation of feed junctions. In the H plane, variable patterns are obtained by exciting from different single ports or from both ports. The maximum gains at 60 GHz were observed at θ equals

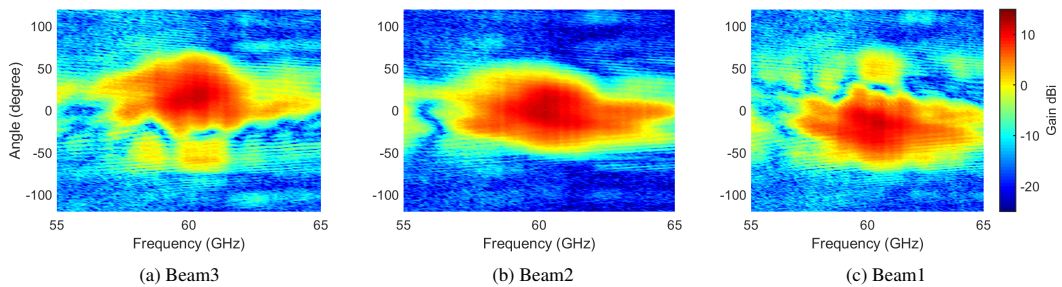


Fig. 8: Experimental measurement of the angular scan of the three generated beams over frequency. Beam numbers follow the naming convention in Figure 1.

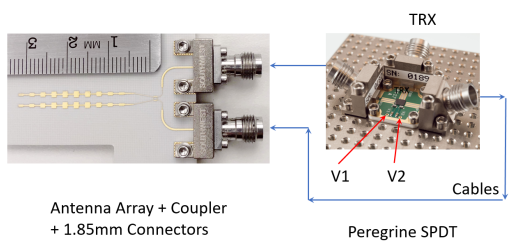


Fig. 9: Top view of the fabricated two row antenna connected to the output of a coupler with an SPDT chip

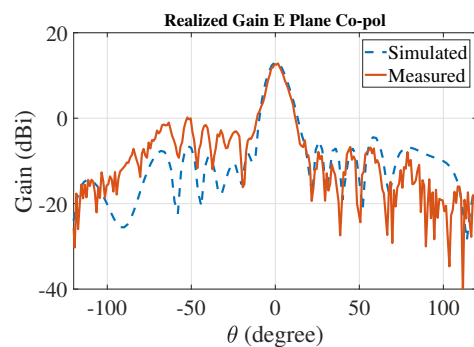


Fig. 11: Comparison of simulated and measured realized gain in E plane of proposed antenna system fed from both ports.

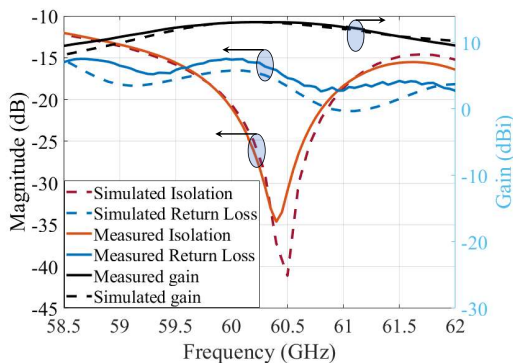


Fig. 10: (Left Axis) S parameter comparison between simulation and measurements of final design showing the isolation between two input ports and the return loss; (Right Axis) Realized gain over the frequency range. It has a gain peak at 60.2 GHz

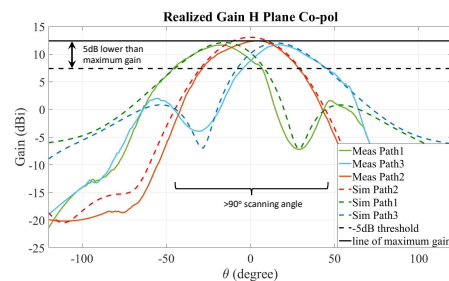


Fig. 12: Comparison of simulated and measured three possible radiation patterns in H plane of proposed antenna system. It is obvious that a phase shift of $\pm 90^\circ$ causes a beam shift by $\pm 22^\circ$. Also, beam scanning angle greater than 90° when the threshold set to be 5 dB lower than maximum gain.

22° , 0° and -22° . The angular coverage and frequency response of the antenna system was measured and presented in Figure 8.

The low-cost ENIG coating helps to protect the copper from being corroded. However, due to the existence of nickel and significant skin-effect in mmWave bands, the conductive loss becomes much higher than it is in pure copper. HFSS simulations shows the gain decrease when adding a nickel layer on top of copper traces. As seen from Table I, while simulated and measurement results match, there is almost 3dB loss when comparing the cases that copper is coated or not. We believe, if using hard gold coating, that the maximum gain of the proposed antenna array can be at least 16 dBi.

5 Conclusion

This paper provides simulation and anechoic-chamber measurement results for our low cost switched-beam antenna array at 60 GHz. The antenna has been designed to serve in a 5G mobile handset in the 60 GHz band. The designed antenna is capable of switching among 3 beams. Two of the beams are generated by feeding through one port of the 2×10 antenna array while the third beam is generated through feeding both antenna arrays to allow a third beam. Antenna switching feature that this antenna configuration provides can be used to

Table 1 Comparison of Simulated and Measurement results with and without ENIG

R2.5:	Simulation with pure copper	Simulation with ENIG	Fabricated with ENIG
1 × 10 antenna	14.5 dBi	12.3 dBi	12.14 dBi
State 1 or 3	16.4 dBi	13.12 dBi	12.93 dBi
State 2	15.6 dBi	12.26 dBi	12.20 dBi

perform wide beam scanning during initial beam search or during handover process in a 5G enabled cellular network.

Acknowledgment

This work was supported by U. S. Office of Naval Research (ONR) under award number N00014-16-1-2037.

6 References

- Rappaport, T.S., Sun, S., Mayzus, R., Zhao, H., Azar, Y., Wang, K., et al.: 'Millimeter wave mobile communications for 5g cellular: It will work!', *IEEE Access*, 2013, **1**, pp. 335–349
- Shafi, M., Molisch, A.F., Smith, P.J., Haustein, T., Zhu, P., Silva, P.D., et al.: '5G: A Tutorial Overview of Standards, Trials, Challenges, Deployment, and Practice', *IEEE Journal on Selected Areas in Communications*, 2017, **35**, (6), pp. 1201–1221
- Hong, W., Jiang, Z.H., Yu, C., Zhou, J., Chen, P., Yu, Z., et al.: 'Multibeam Antenna Technologies for 5G Wireless Communications', *IEEE Transactions on Antennas and Propagation*, 2017, **65**, (12), pp. 6231–6249
- Han, S., I. I. C., Xu, Z., Rowell, C.: 'Large-scale antenna systems with hybrid analog and digital beamforming for millimeter wave 5G', *IEEE Communications Magazine*, 2015, **53**, (1), pp. 186–194
- García-Rodríguez, A., Venkateswaran, V., Rulikowski, P., Masouros, C.: 'Hybrid Analog-Digital Precoding Revisited Under Realistic RF Modeling', *IEEE Wireless Communications Letters*, 2016, **5**, (5), pp. 528–531
- Venkateswaran, V., Pivit, F., Guan, L.: 'Hybrid RF and Digital Beamformer for Cellular Networks: Algorithms, Microwave Architectures, and Measurements', *IEEE Transactions on Microwave Theory and Techniques*, 2016, **64**, (7), pp. 2226–2243
- SeyyedEsfahlan, M., Üztürk, E., Kaynak, M., Tekin, I.: '77-GHz Four-Element Phased-Array Radar Receiver Front End', *IEEE Transactions on Components, Packaging and Manufacturing Technology*, 2016, **6**, (8), pp. 1162–1173
- Tseng, C.H., Chen, C.J., Chu, T.H.: 'A Low-Cost 60-GHz Switched-Beam Patch Antenna Array With Butler Matrix Network', *IEEE Antennas and Wireless Propagation Letters*, 2008, **7**, pp. 432–435
- Yang, Q.L., Ban, Y.L., Lian, J.W., Yu, Z.F., Wu, B.: 'SIW Butler Matrix with Modified Hybrid Coupler for Slot Antenna Array', *IEEE Access*, 2016, **4**, pp. 9561–9569
- Liu, Y., Bshara, O., Tekin, I., Dandekar, K.R.: 'A 4 by 10 series 60 GHz microstrip array antenna fed by butler matrix for 5G applications'. In: 2018 IEEE 19th Wireless and Microwave Technology Conference (WAMICON), (2018), pp. 1–4
- Ding, K., Fang, X., Wang, Y., Chen, A.: 'Printed Dual-Layer Three-Way Directional Coupler Utilized as 3 × 3 Beamforming Network for Orthogonal Three-Beam Antenna Array', *IEEE Antennas and Wireless Propagation Letters*, 2014, **13**, pp. 911–914
- Odrobina, S., Staszek, K., Wincza, K., Gruszczynski, S.: 'Broadband 3 × 3 Butler Matrix'. In: 2017 Conference on Microwave Techniques (COMITE), (2017), pp. 1–5
- Pozar, D.M.: 'Microwave engineering, 4th edition', *Wiley Global Education*, 2011,
- : 'Peregrine Semiconductor PE42525 specification', <https://www.psemi.com/pdf/datasheets/pe42525ds.pdf>, 2016,